Pipeline Flange Loose Bolt Localization Technology Based on Waveform Correlation Coefficient

Cong Yu[1,2], Peng Cheng[1,2,*], Chenxi Shao[1,2]
[1]*China Academy of Machinery Science and Technology. Beijing, China*
[2]*Yanqi Lake Institute of Basic Manufacturing Technology Research (Beijing) Co., Ltd., Beijing, China*
**Corresponding Author*

Abstract: To address the challenge of locating bolt looseness in pipeline flanges equipped with sealing gaskets, this paper proposes a detection method based on stress wave principles combined with deep learning. Vibration signals were collected under various bolt loosening conditions at different excitation points on the flange. The overall waveform correlation coefficient and segmental waveform correlation coefficients of the signals were calculated to construct a feature dataset, and a Support Vector Machine (SVM) model was employed to identify the positions of loosened bolts. Experimental results demonstrate that when excitation points are selected near the sensor or far from the sensor, the waveform correlation coefficients across different time domains effectively reflect variations in the location of loosened bolts, achieving high recognition accuracy. This method provides a feasible technical approach for accurately locating bolt looseness in pipeline flanges.

Keywords: Flange Bolt Looseness; Stress Wave; Waveform Correlation Coefficient; Support Vector Machine; Structural Health Monitoring

1. Introduction

Flange connections serve as critical load-bearing structures in wind turbine towers, pipeline transportation, bridge engineering, and related fields. The issue of bolt loosening in such connections has consistently been a research focus in structural health monitoring. In recent years, scholars both domestically and internationally have conducted extensive research on this topic, achieving notable progress in areas such as the electromechanical impedance method, ultrasonic guided wave method, piezoelectric sensing technology, and the integrated application of machine learning.

Jiang et al. [1] conducted systematic experimental monitoring of high-strength bolt loosening in flange connections using the piezoelectric wave method. They designed a flange connection specimen containing four high-strength bolts and set up five conditions: a healthy state and states with one to four loosened bolts. Three methods—time-domain analysis, frequency-domain analysis, and wavelet packet energy analysis—were employed to comprehensively assess the degree of damage. The results indicated that as the tightness of the flange connection decreased, the amplitudes of both time-domain and frequency-domain signals gradually diminished, accompanied by a reduction in wavelet packet energy. This provided a reliable basis for the quantitative assessment of multi-bolt loosening.

Yan et al. [2] proposed a method for monitoring bolt loosening in flange joints based on time reversal technology. This study established a correlation between the peak value of the focused stress wave signal and the bolt preload. In the experimental design, one piezoelectric ceramic sensor was attached to the bolt cap as an actuator, while another was attached to the flange plate as a sensor, using the peak value of the focused stress wave signal as the monitoring indicator.

Gao et al. [3] employed an improved YOLOv8 network, introducing a Mobile ViT backbone to balance local texture features. This was combined with large separable convolution kernels, attention mechanisms, and multi-scale feature fusion to achieve high-precision detection of small bolts in complex backgrounds. For angle estimation, a training-free feature detection and matching process was adopted. Even under conditions of reflection, blurring, or changes in viewing angle, the success rate of angle estimation remained between 85% and 93%, with an average error close to 1 degree.

I. Kajiwara et al. [4] proposed a non-contact laser excitation detection method for identifying bolt loosening through high-frequency vibration measurements. This method uses a laser to excite the target structure, generating high-frequency vibrations, and measures the response characteristics to assess the fastening state of bolts without direct contact.

Huang et al. [5] introduced a flange model where connection stiffness varies with position by installing gaskets of different thicknesses at different bolt locations. By analyzing the frequency shift sequence characteristics extracted from coupled impedance spectra, they successfully identified the position of loosened bolts. The study found that the correlation between frequency shift sequences corresponding to loosening at different bolt positions was low, while the sequences were highly correlated with the degree of loosening. Thus, loosening localization could be achieved through calibrated sequence matching.

Current research on detecting bolt loosening in flanges predominantly focuses on flat flanges without sealing gaskets, based on the principle of reduced bolt preload leading to changes in local axial stiffness. However, research on sealed flanges with gaskets remains limited. To achieve the localization of bolt loosening in pipeline sealing flanges, this paper proposes a method based on stress wave principles and deep learning. The method uses the waveform correlation coefficient as an evaluation metric to identify the location of loosened bolts. Vibration signals are collected by striking the flange under various bolt loosening conditions. The overall waveform correlation coefficient and segmental waveform correlation coefficients are calculated, and an SVM model is trained to localize loosened bolts. This provides a technical approach for achieving accurate and efficient diagnosis of bolt loosening in pipeline flanges.

2. Principle of Bolt Looseness Detection Based on Stress Waves

Stress waves are phenomena where stress and strain disturbances propagate as waves in deformable solid media. Their propagation characteristics are closely related to the medium properties and loading conditions. Elastic gaskets are widely used in impact protection, vibration reduction, and noise attenuation, and their efficiency in transmitting stress waves directly determines their buffering performance. Transmission efficiency is primarily manifested in wave velocity and attenuation characteristics, which have a certain mathematical relationship with the elastic properties of the gasket.

For one-dimensional longitudinal waves in an infinitely long elastic rod, the wave velocity is determined by the material density and elastic modulus.

$$c = \sqrt{\frac{E}{\rho}} \tag{1}$$

Here, c represents the wave velocity, E is the elastic modulus, and ρ is the material density. This formula indicates that the greater the elastic modulus and the smaller the density, the faster the wave velocity.

In practical applications, gaskets are typically in a state of pre-compression. According to incremental elasticity theory [6], the relationship between wave velocity under pre-strain and wave velocity in the initial state is given.

$$\frac{c(\varepsilon_0)}{c_0} = 1 + \frac{1}{2}\left(\frac{C_3}{E}\right)\varepsilon_0 \tag{2}$$

Here, ε_0 represents the pre-strain, and C_3 represents the third-order elastic constant. Research [7] indicates that the wave velocity of stress waves within a material is influenced by the pre-strain magnitude. In a pipeline flange, when a bolt loosens, the clamping force in that bolted region decreases, reducing the pressure on the gasket and consequently the pre-strain magnitude, thereby affecting the wave velocity of stress waves within the gasket.

Elastic gaskets are typically made of polymer materials exhibiting viscoelastic properties. Using a constitutive model where a Maxwell model is connected in parallel with an elastic element [8], the complex modulus can be expressed.

$$E^*(\omega) = E_\infty + \frac{i\omega\eta E_0}{E_0 + i\omega\eta} \tag{3}$$

Here, E_∞ represents the high-frequency limit modulus, E_0 is the static modulus, and η is the viscosity coefficient. Decomposing the formula into real and imaginary parts yields.

$$E^*(\omega) = E' + iE'' \tag{4}$$

$$E' = E_\infty + \frac{\omega^2\eta^2 E_0}{E_0^2 + \omega^2\eta^2} \tag{5}$$

$$E'' = \frac{\omega\eta E_0^2}{E_0^2 + \omega^2\eta^2} \tag{6}$$

Where E' represents the storage modulus and E'' represents the loss modulus.

When the wavelength of the stress wave is comparable to the lateral dimensions of the gasket (or rod), lateral inertial motion causes geometric dispersion of the wave. The Rayleigh-Love theory introduces a correction term to the classical one-dimensional wave equation to account for the effect of lateral inertia [9].

$$E^{*}\frac{\partial^2 u}{\partial x^2}+\rho\nu^2k^2\frac{\partial^4 u}{\partial x^2\partial t^2}=\rho\frac{\partial^2 u}{\partial t^2} \quad (7)$$

Here, ν represents Poisson's ratio, and k represents the radius of gyration of the cross-section. Assuming a simple harmonic wave solution.

$$u(x,t)=Ue^{i(\gamma x-\omega t)} \quad (8)$$

where γ is the complex propagation coefficient. Substituting the simple harmonic wave solution into the wave equation yields the characteristic equation.

$$-E^{*}\gamma^2-\rho\nu^2k^2\gamma^2\omega^2+\rho\omega^2=0 \quad (9)$$

Let

$$\gamma=\alpha+i\beta \quad (10)$$

where α is the phase coefficient, affecting wave velocity, and β is the attenuation coefficient, affecting the amplitude decay of the wave.
Substituting the complex modulus yields.

$$\alpha=\omega\sqrt{\frac{\rho}{E'+\rho\nu^2k^2\omega^2}} \quad (11)$$

$$\beta=\frac{\omega}{2c}\cdot\tan\delta=\frac{\omega}{2c}\cdot\frac{E''}{E'} \quad (12)$$

From the above formulas, it is evident that changes in the elastic properties of the material lead to variations in wave velocity and energy attenuation of stress waves within the material. In a pipeline sealing flange, when a bolt loosens, the elastic modulus of the gasket changes with the applied pressure, subsequently affecting the propagation characteristics of waves within the gasket.

3. Experimental Setup and Data Acquisition

3.1 Test Bench Construction

A test bench for detecting bolt loosening in flanges was constructed, as shown in Figure 1. The flange is a PN10, DN80 integral flange, secured with eight M16 bolts with an initial tightening torque of 75 Nm. The sealing gasket is a spiral-wound gasket. Bolts at different positions on the flange were labeled 1 to 8. The sensor was placed on the lower flange near bolt No. 1. A force hammer fitted with an aluminum alloy hammerhead was used as the excitation source, applying a striking force of 1000 N at points located between bolts on the upper flange. Based on the symmetry of the flange, four positions (A, B, C, D) were selected as excitation points for the experiment. The bolt labeling and excitation point positions are shown in Figure 2.

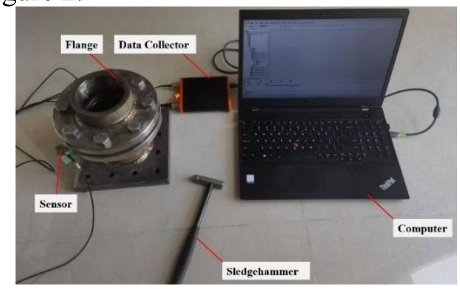

Figure 1. Flange Bolt Looseness Detection Test Bench

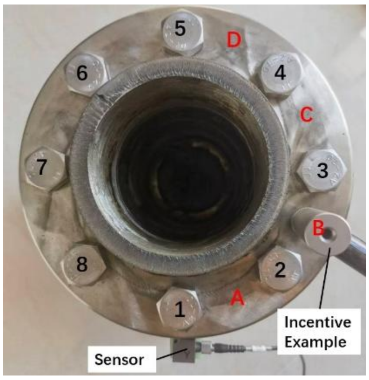

Figure 2. Bolt Labeling and Excitation Point Positions

3.2 Experimental Procedure

To investigate the performance of this detection method for early-stage bolt loosening, the tightening torque for the loosened condition in this experiment was set to 62.5 Nm. First, a digital torque wrench was used to tighten all bolts on the flange to 75 Nm. The system sampling frequency was set to 64000 Hz, with a sampling time of 0.025 s. ten excitations were performed at points A through D to acquire vibration data under the fully tightened condition. After each excitation, the magnitude of the striking force was checked to ensure it remained within an error of 50 N, preventing significant differences in vibration signals due to variations in impact force that could affect subsequent analysis.

After data acquisition, bolt No. 1 was completely loosened and then retightened to 62.5 Nm to simulate a loosened condition. Ten excitations were performed at points A through D to acquire vibration data under the condition with bolt No. 1 loosened. After completing this step, bolt No. 1 was retightened to 75 Nm, and bolt No. 2 was loosened. This process was repeated until vibration data were acquired for all eight bolts under loosened conditions.

4. Results and Analysis

4.1 Experimental Results Analysis

Figure 3 shows time-domain comparisons of vibration signals under various bolt loosening conditions at excitation points A through D.

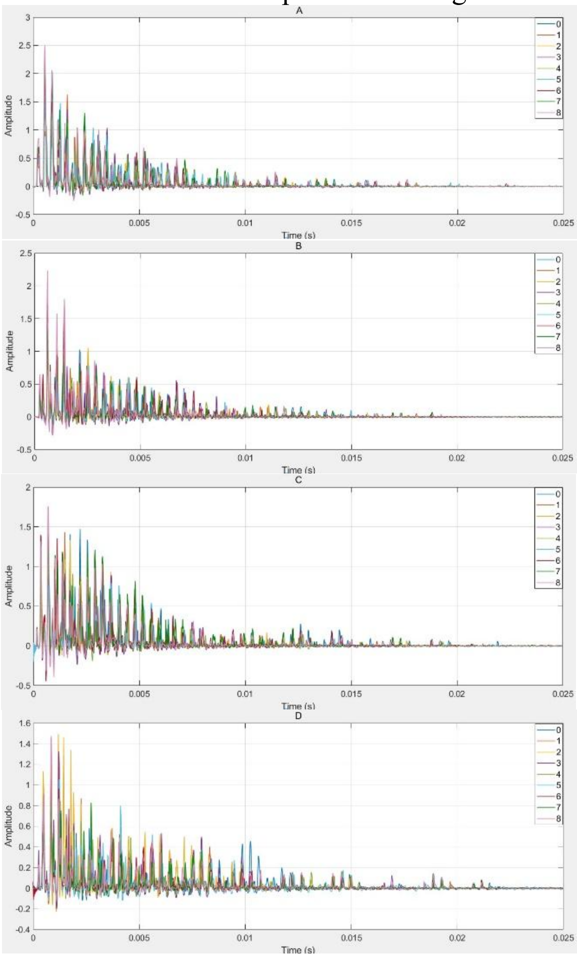

Figure 3. Time-domain Comparison of Vibration Signals under Different Conditions

Analysis of the time-domain figures reveals that when the excitation point is the same, variations in the position of the loosened bolt result in different waveform changes in the acquired vibration signals. According to the breathing effect theory, bolt loosening causes periodic "opening-closing" motion of the contact interface under dynamic excitation. This nonlinear behavior modulates the stress waves in the bolted connection structure, leading to changes in the waveform and frequency spectrum [10]. Additionally, due to the Poisson's ratio of the gasket material, particles undergo not only axial motion but also lateral motion during propagation, causing waveform distortion. The degree of this distortion varies with the propagation distance and the energy of the stress wave. Based on geometric dispersion theory, waves of different frequencies travel at different speeds, causing an initially sharp stress wave to broaden and decrease in amplitude after propagating a distance x [11]. Therefore, under identical excitation conditions, variations in the position of the loosened bolt on the flange lead to different degrees of waveform alteration in the acquired vibration signals.

4.2 Method for Locating Loosened Bolts Based on Waveform Correlation Coefficient

4.2.1 Waveform correlation coefficient

Based on the analysis of the impact of bolt loosening in pipeline flanges on signal waveforms, a method for locating loosened bolts in flanges using the waveform correlation coefficient is proposed. The waveform correlation coefficient is a parameter that measures the similarity between two signal waveforms, calculated as follows.

$$r = \frac{\sum_{i=1}^{n}(x_i - \bar{x})(y_i - \bar{y})}{\sqrt{\sum_{i=1}^{n}(x_i - \bar{x})^2} \cdot \sqrt{\sum_{i=1}^{n}(y_i - \bar{y})^2}} \tag{13}$$

Here, n is the signal length, x_i and y_i are the data points of the signals at the i, and $\bar{x}$ and $\bar{y}$ are the means of the signals. The closer this coefficient is to 1, the more similar the two signal waveforms; the closer it is to 0, the greater the difference.

The vibration data obtained from the experiments were divided into four groups based on excitation points. One data point was randomly selected from the non-loosened condition within each group as a reference. The waveform correlation coefficients for data under different bolt loosening conditions were calculated. Figure 4 shows the waveform correlation coefficients under different conditions for each excitation point.

Analysis of Figure 4 shows that under the same excitation conditions, the waveform correlation coefficients vary across different bolt loosening conditions. However, the coefficients for some conditions are relatively close to each other. In these cases, the overall waveform similarity between the vibration signal and the signal from the non-loosened condition is approximately the same, making it difficult to distinguish these conditions using only this metric. Nevertheless, when the position of the loosened bolt differs, the propagation path length of the stress wave before passing through the region of the loosened bolt varies, resulting in different energy losses, different degrees of distortion, and different levels of geometric dispersion [11]. Consequently, under different conditions, the waveform of the vibration signal within a specific time segment may exhibit varying degrees of difference. Based on this principle, a method for locating loosened bolts by calculating waveform correlation coefficients over different time intervals is proposed.

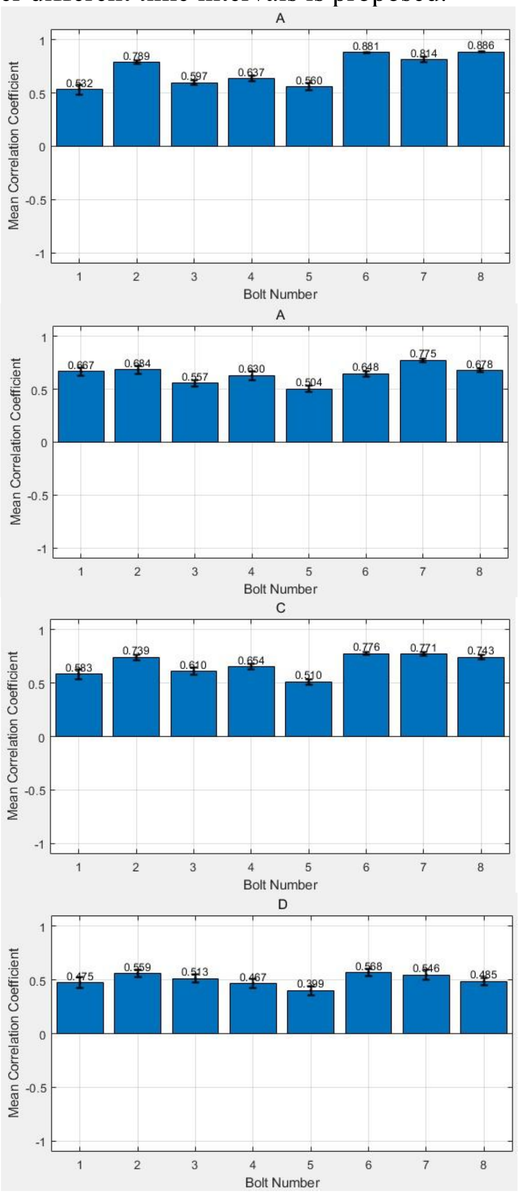

Figure 4. Waveform Correlation Coefficients for Different Conditions at Each Excitation Point

4.2.2 Dataset partitioning and model training

The Support Vector Machine (SVM), as a classic supervised learning algorithm, is widely used in classification and regression analysis. The core idea of the algorithm is to construct an optimal separating hyperplane that effectively divides different classes of samples in the feature space while maximizing the classification margin. This hyperplane is determined solely by a few sample points closest to it—the support vectors—reflecting the superiority of SVM within the framework of structural risk minimization. SVM is capable of handling high-dimensional data and can effectively address nonlinear classification problems by introducing kernel techniques, thus demonstrating good generalization performance and robustness.

The vibration data acquired at excitation point A in the experiment described in Section 3 were divided into nine groups based on loosening conditions. One data point was randomly selected from the non-loosened condition data as the reference for waveform correlation coefficient calculation, while the remaining eight groups served as the data for calculation. These were randomly partitioned into training and test sets in a 7:3 ratio. As shown in Figure 3, the vibration signals obtained in this experiment exhibit significant waveform changes within the first 0.0125 s. To reduce computational cost, only the data within the first 0.0125 s of the signals were used for waveform correlation coefficient calculation. Using intervals of 0.00125 s, both the reference data and the data points in the calculation set were divided into 10 time segments. The waveform correlation coefficient for each time interval was calculated. An SVM model was trained and tested using the dataset based on the above features. To avoid chance, 50 repeated random experiments were conducted. The confusion matrices for bolt loosening position detection at each excitation point are shown in Figure 5.

Based on the analysis of the results, when excitation was applied at points A, C, and D, the detection accuracy for bolt loosening localization based on waveform correlation coefficients in different time domains was high. When the excitation point was B, the method showed poor recognition capability for loosening of bolts No. 1 and No. 2. This might be because, when exciting at point B, the path length of the stress wave passing through the loosened bolt region (for bolts No. 1 and No. 2) to the sensor is relatively short. Consequently, the distortion and geometric dispersion effects on the signal are relatively similar, leading to higher waveform similarity under these two conditions and increasing the likelihood of misclassification. Therefore, this bolt loosening detection scheme should select excitation points either near the sensor or relatively far from the sensor.

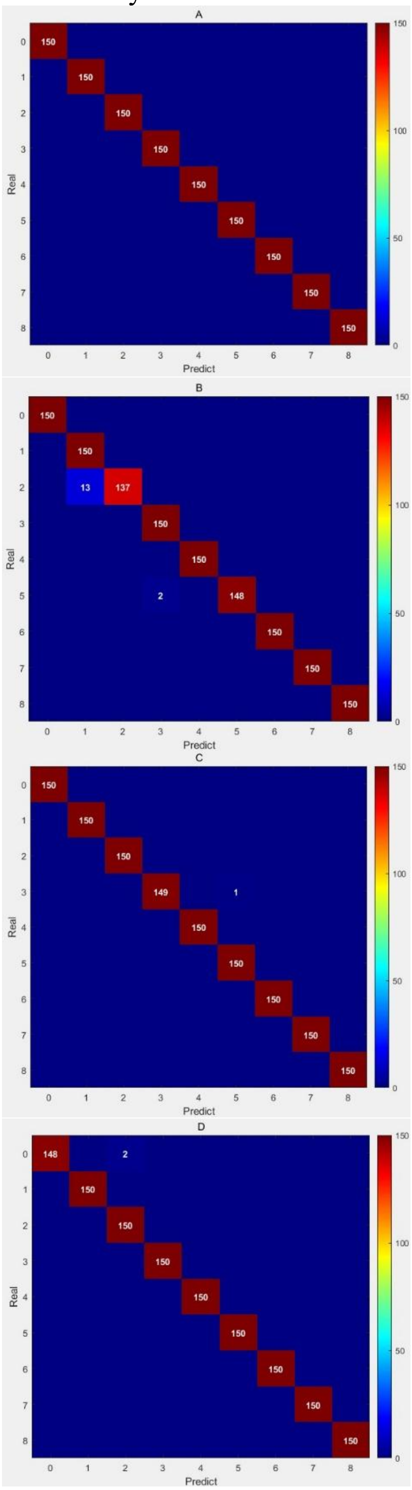

Figure 5. Confusion Matrices for Bolt Loosening Position Identification at Each Excitation Point

5. Conclusion

To achieve the localization of bolt looseness in pipeline sealing flanges equipped with sealing gaskets, this paper proposes a detection technique based on stress wave principles, utilizing the waveform correlation coefficient. Experimental analysis shows that under identical excitation conditions, the overall waveform correlation coefficient of the signal varies with the position of the loosened bolt. However, the waveform correlation coefficients for some bolt loosening conditions are relatively close, making it difficult to reliably identify the location of the loosened bolt using this single metric. Based on the theory of geometric dispersion of stress waves, the method of using waveform correlation coefficients within different time segments of the signal as indicators for detecting the position of loosened bolts is proposed. A dataset of signals under bolt loosening conditions was acquired experimentally, and SVM was employed for bolt loosening detection testing. The test results demonstrate that when excitation points are selected near the sensor or far from the sensor, the proposed method can accurately identify the position of loosened bolts in pipeline flanges.

References

[1] Jiang Tianyong, Fang Lin, Liang Shijie. Experimental Study on Monitoring of High-Strength Bolt Loosening Damage in Flange Connections Based on Piezoelectric Ceramics. Journal of China & Foreign Highway, 2022(001): 042.

[2] Yan Zunhao, Xu Jing, Zhang Duan, et al. Research on Bolt Loosening Monitoring of Steel Tower Flange Joints Based on Time Reversal Technology. Journal of Qingdao University of Technology, 2025, 46(2).

[3] Gao Y, Zhou S, Li M. Real-Time Flange Bolt Loosening Detection with Improved YOLOv8 and Robust Angle Estimation. Sensors (Basel). 2025 Oct 6;25(19):6200.

[4] Kajiwara I, Miyamoto D, Hosoya N, et al. Loose Bolt Detection by High Frequency Vibration Measurement with Non-Contact Laser Excitation. Journal of System Design & Dynamics, 2011, 5(8): 1559-1571.

[5] Huang H, He Q. Bolt looseness localization with connection-stiffness-varying flange. Smart Materials & Structures, 2024(9): 33.

[6] Mohabuth M, Kotousov A, Ng C T. Large acoustoelastic effect for Lamb waves propagating in an incompressible elastic plate. The Journal of the Acoustical Society

of America, 2019, 145(3): 1221-1229.

[7] Bo, Song, Brett, et al. Experimental Measurement and Analysis of Stress/Shock Wave Propagation Speed through Pre-strained Silicone Foam Pads under Lateral Confinement. Journal of Dynamic Behavior of Materials, 2019, 5(2): 170–179.

[8] Gopalakrishnan S. Wave Propagation in Viscoelastic Waveguides. Elastic Wave Propagation in Structures and Materials, 2022: 129-156.

[9] Aleyaasin M, Harrigan J J. Wave dispersion and attenuation in viscoelastic polymeric bars: Analysing the effect of lateral inertia. International Journal of Mechanical Sciences, 2010, 52(5): 754-757.

[10]Li X X, Li D, Ren W X, et al. An RFE-aided Transformer-SVM framework for multi-bolt connection loosening identification using wavelet entropy of vibro-acoustic modulation signals. Advances in Structural Engineering, 2025, 28(1).

[11]Yang Hongsheng, Li Yulong, Zhou Fenghua. Propagation Process and Geometric Dispersion of Trapezoidal Stress Pulses in Elastic Rods. Chinese Journal of Theoretical and Applied Mechanics, 2019, 51(6): 10.

